Quantum Entrained Measurements

Ole Steuernagel

School of Physics, Astronomy and Mathematics, University of Hertfordshire, Hatfield, AL10 9AB, UK *
(Dated: June 3, 2011)

A new response mode of quantum systems, repeatedly interrogated by quantum probe particles, is introduced: *quantum entrainment*. Quantum entrainment is shown to arise in an interferometric scheme for the creation of Schrödinger cat states of mechanical oscillators, using a quantum mirror kicked by free photons. This scheme features ultra-fast preparation with immediate detection and should allow for the observation of signatures of spatial superpositions in a massive macroscopic system at non-zero temperatures. It is sensitive and yet robust against thermal noise, displacement and movement, mirror imperfections and the measurements' back-actions.

Heisenberg's uncertainty principle enforces that quantum measurements' back-actions leave traces in an observed system [1, 2]. Although their random nature can be useful (back-action protects quantum cryptography protocols from eavesdropping and it can help to cool tiny mirrors [3]), the traces are usually detrimental and back-action avoidance has been researched intensively [4]. Uncontrollable measurement back-actions give rise to loss of coherence (decoherence [5]) which hampers us when building quantum computers, running sensitive interferometers for gravitational wave detection, or synthesizing Schrödinger cat states of classical objects.

Here we show that measurement back-actions can be restricted and harnessed yielding a fruitful and stabilizing influence. Several probe particles interact with a quantum system and are subsequently detected; the traces they leave in the system modifies the future behaviour of following probe particles. These repeated interactions can prepare the system in a desirable quantum state and the features of that quantum state can show up in modified measurement statistics of future probe particles. An initially unbiased setup can thus become skewed by repeated quantum interrogation. The system and its probe particles have become *quantum entrained*.

Quantum entrainment allows us to create otherwise difficult-to-realize quantum states. Its self-reinforcing nature stabilizes the prepared states' desirable features in a robust fashion, and it allows us to detect the non-classical nature of the created state while leaving the state intact.

We consider a Michelson-Morley interferometer in which the central, two-sided mirror is quantum-delocalized in the x-direction –perpendicular to its reflecting surfaces [3, 6, 7], see Fig. 1. The quantum mirror's wavefunction is described by its center-of-mass density matrix $\rho(x, \xi)$ for which we want to assume that it has a coherent extension of a few tens of nanometers (this can, for example, be achieved through a ballistic expansion of a tightly squeezed and cooled mirror [8] which is suddenly set free [9]).
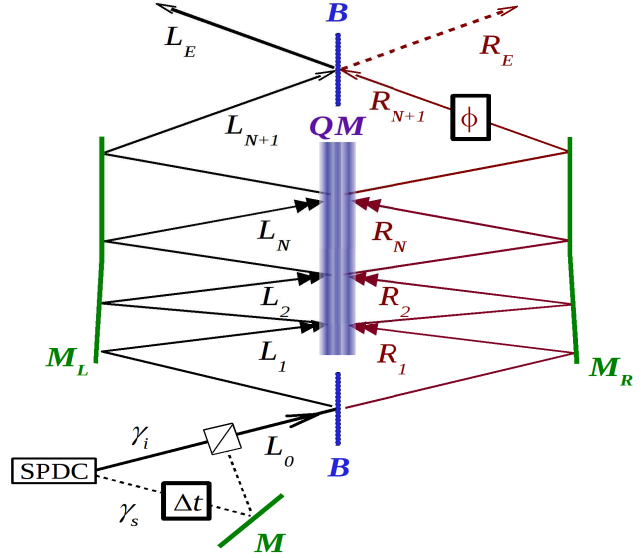
FIG. 1: Setup for interferometric preparation and read-out of the state of a quantum mirror (QM). The initial photon γ_i enters the interferometer through mode L_0, gets split into equal partial waves by a balanced beam splitter B and traverses the interferometer via successive paths L_1, L_2, etc. or alternatively via paths R_1, etc. Every time it is reflected by the quantum mirror it imparts a momentum kick and thus prepares the mirror in a momentum superposition state (the corresponding modes are symbolized by folded double-arrows). A phase shifter ϕ allows us to scan the photons' interference patterns. The final balanced beam mixer B removes 'which-path' information; when the photon gets detected in mode L_E or R_E, this measurement projects the mirror into a momentum-superposition state. With an ultra-short time delay, see Eq. (1), a second photon γ_s follows γ_i via a polarizing beam splitter through the interferometer and interrogates the state of the quantum mirror.

In the first step of the entrainment procedure a single photon γ_i, such as those available from spontaneous parametric down-conversion (SPDC) pair-creation processes [10], is sent through the interferometer, entering, say, through port L_0.

In a classical interferometer, the phase-shifter ϕ can be

set such that this photon will exit through port L_E with certainty since destructive interference renders port R_E dark. With a quantum delocalized central mirror, however, this interference pattern gets washed out and photons will exit through port R_E as well.

We want to use one photon at-a-time arrangements, the next photon should interact with the quantum mirror after the previous has passed. The delay time between any two photons is therefore constrained by

$$\Delta t > \delta t + \frac{D(N-1)}{c} \, , \qquad (1)$$

here $\delta t \approx 100$ fs is the photons' coherence time [10] and D the distance they travel between two quantum mirror interactions. Note that for single bounce setups ($N = 1$) the interaction time for m photons is thus bound by $T_m \approx m \cdot \delta t$ and we can generate and interrogate a momentum-superposition state repeatedly on the picosecond timescale. This is in marked contrast to the "standard approach" of confining the light inside a cavity [11–14].

For the formal analysis we need to determine the bosonic light-field operators $\hat{L}_E$ and $\hat{R}_E$ at the exit ports in terms of those at the entrance ports $\hat{L}_0$ and $\hat{R}_0$ (we will leave $\hat{R}_0$ empty, see Fig. 1)

$$\begin{pmatrix} \hat{L}_E \\ \hat{R}_E \end{pmatrix} = \mathbf{B}\mathbf{P}_{N+1}\mathbf{K}_N\mathbf{P}_N \cdot \ldots \cdot \mathbf{K}_2\mathbf{P}_2\mathbf{K}_1\mathbf{P}_1\mathbf{B} \begin{pmatrix} \hat{L}_0 \\ \hat{R}_0 \end{pmatrix} \, . (2)$$

The unitary 2×2 matrices $\mathbf{B}$, $\mathbf{P}$ and $\mathbf{K}$ describe balanced mirrors, photon propagators and kick operators, respectively. Specifically, $\mathbf{B} = \mathbf{S}(\frac{\pi}{4})$ is a special case of a lossless splitter $\mathbf{S}$ with reflection probability $\cos(\theta)^2$, namely

$$\mathbf{S}(\theta) = \begin{pmatrix} \cos(\theta) & i\sin(\theta) \\ i\sin(\theta) & \cos(\theta) \end{pmatrix} \, . \qquad (3)$$

The photon propagators

$$\mathbf{P}_j = \begin{pmatrix} P_{L,j} & 0 \\ 0 & P_{R,j} \end{pmatrix} \qquad (4)$$

account for the path length of mode 'j' including the phase jump due to the reflection by the perfect mirrors M_L and M_R respectively.

The kick operators enact the partial reflection and transmission of photons by the quantum mirror in conjunction with the associated momentum transfer to its center-of-mass density matrix $\rho(x, \xi)$:

$$\hat{\mathbf{K}}_j(\theta) = \begin{pmatrix} \cos(\theta)\,\hat{K}_{L_j}(\hat{x}) & i\sin(\theta) \otimes \mathbb{1} \\ i\sin(\theta) \otimes \mathbb{1} & \cos(\theta)\,\hat{K}_{R_j}(\hat{x}) \end{pmatrix} \, . \qquad (5)$$

With an angle of incidence ϵ the effective photon momentum transfer is $p_\gamma = 2\hbar k \cos(\epsilon)$, where $k = 2\pi/\lambda$ is their wave number and the kick operators in Eq. (5) have the form

$$\hat{K}_{L_j}(\hat{x}) = \exp(\hat{L}_j^\dagger \hat{L}_j \otimes \frac{ip_\gamma \hat{x}}{\hbar}) \, , \qquad (6)$$

$$\text{and} \quad \hat{K}_{R_j}(\hat{x}) = \exp(-\hat{R}_j^\dagger \hat{R}_j \otimes \frac{ip_\gamma \hat{x}}{\hbar}) \, . \qquad (7)$$

The initial density matrix of the system (quantum mirror plus light field) is

$$\varrho(x, \xi; l_0, r_0) = \rho(x, \xi) \frac{(\hat{L}_0^\dagger)^{l_0}(\hat{R}_0^\dagger)^{r_0}|0\rangle\langle 0|\hat{L}_0^{l_0}\hat{R}_0^{r_0}}{l_0! r_0!} \, . \qquad (8)$$

We will from now on assume that only single photons are present at-a-time, i.e. $l_0 = 1$ and $r_0 = 0$. The determination of photon numbers at an output port of the interferometer involves tracing out the quantum mirror and projecting onto that port (here: L_E)

$$\langle \hat{n}_{L_E} \rangle = \langle Tr_{QM}\{\hat{L}_E^\dagger \hat{L}_E \varrho\} \rangle = \langle \int dx \hat{L}_E^\dagger \hat{L}_E \varrho(x, x) \rangle. \qquad (9)$$

Tracing over the field yields an effective kick-operator $\mathcal{K}$ acting on the density matrix ρ. For example, for the setup of Fig. 1 with a single bounce off the mirror ($N = 1$) and assuming a photon enters through path L_0 and is found to exit through port L_E we have (with $\epsilon = 0$)

$$\mathcal{K}_{L_E} = \left[\sin(\theta)\cos(\frac{\phi}{2}) - i\cos(\theta)\sin(2kx - \frac{\phi}{2})\right]$$
$$\times \left[\sin(\theta)\cos(\frac{\phi}{2}) + i\cos(\theta)\sin(2k\xi - \frac{\phi}{2})\right] \, . (10)$$

For simplicity we write $K_{L_E} = K_L$, then, similarly, $\mathcal{K}_R = \mathcal{K}_L(\phi \mapsto \phi - \pi)$.

According to Eq. (1) the time of interaction between all successive photons and the quantum mirror are very short, all reference to the time evolution of the quantum mirror is therefore absent in our expressions for $\mathcal{K}$.

Since the quantum mirror's density matrix ρ changes in response to the port in which the exiting photon is detected, we represent the history associated with varying experimental outcomes through a multi-index, namely, we write down the ports L or R in which the exiting photons are registered:

$$\rho_{LRLL}(x, \xi) = (\mathcal{K}_L \rho_{RLL})(x, \xi)$$
$$= (\mathcal{K}_L \mathcal{K}_R \mathcal{K}_L \mathcal{K}_L \rho_0)(x, \xi) \, , \qquad (11)$$

for example, describes the mirror's density matrix when the fourth photon is seen in the left port after the first two were detected there as well, but the third exited to the right.

The initial quantum mirror density matrix ρ_0 is normalized: $\int dx \, \rho_0(x, x) = 1$, this is not true for density matrices conditioned on measurements. Only all conditional density matrices taken together are normalized since, for $x = \xi$, we have

$$\mathcal{K}_L + \mathcal{K}_R = 1 \, , \qquad (12)$$

in other words, the integrated conditional density matrices carry the relative weights for the occurrence of certain experimental outcomes: $p_H = \int dx \, \rho_H(x, x)$. Here H is the history label which denotes the occurrence of a specific run, such as $H = RLL$ –in example (11). We are

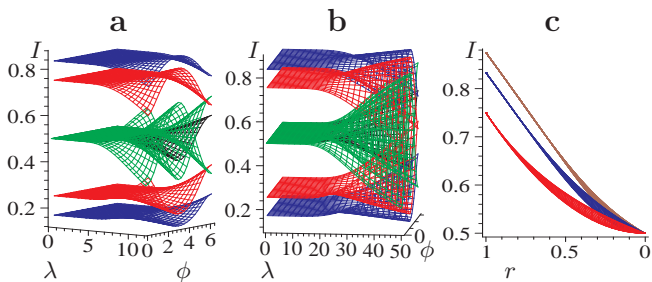FIG. 2: Intensity distribution $I(\lambda, \phi)$ for single-bounce setup ($N = 1$) of a Gaussian quantum mirror (initial density matrix for a fully coherent state $\rho_0(x,x) = \exp(-x^2/\sigma^2)/(\sigma\sqrt{\pi})$, coherent spread $\sigma = 1$) with perfect reflectivity $r = 1$. (a) For small values of wavelength λ interference is washed out whereas for values of $\lambda/\sigma > 8$ it shows: I_L and I_R (green graphs centered around 0.5). Detection of second $I_{L,L}$ (red, centered on 0.75) and third photon $I_{L,LL}$ (blue, centered on $5/6 \approx 0.83$) shows strong *photon entrainment*. For mixed histories the weights are strongly reduced $I_{R,L}$ (red, at 1/4), $I_{R,LL}$ (blue curve at 1/6) and $I_{R,LR}$ (black). (b) Same plot as (a) for triple-bounce case $N = 3$. The effective resolution of the probe particles rises to $\Lambda \approx \lambda/(3 \cdot 8)$: above $\lambda/\sigma \approx 24$ the quantum washout of the interference pattern diminishes. (c) Same plot as (a) for $I_{L,L}$, $I_{L,LL}$ and $I_{L,LLL}$, for ($\lambda \ll \sigma$), as a function of decreasing mirror reflectivity r. The widths of the curves indicate variation with change of the phase angle ϕ (not shown). The entrainment persists for imperfect mirrors.

FIG. 3: Probability densities $\rho(x,x)$ of quantum mirror in initially Gaussian state with $\sigma = 1$, $\lambda = 1$ and symmetric setup, $\phi = 0$. Thin solid black line. (a) Single-bounce setup ($N = 1$), after first photon has been detected: ρ_L and ρ_R (solid red and green line); similarly after detection of second ρ_{LL}, ρ_{RR} and third photon ρ_{LLL}, ρ_{RRR} (red and green dashed and dotted lines). For mixed measurement-histories the weights are strongly reduced $\rho_{RL} = \rho_{LR}$ (green-red) and ρ_{RLR} (blue dash-dotted line) this clearly demonstrates *quantum entrainment*. (b) Double-bounce setup ($N = 2$), compared to (a) the imprint wavelength has halved. (c) Same as (a) for an imperfect quantum mirror with reflectivity $r = 60\%$.

thus led to define the momentary spatial quantum mirror probability density

$$\alpha_{L,H}(x) = \frac{\rho_{LH}(x,x)}{p_H} , \qquad (13)$$

which, when integrated over, yields the probability I to observe a photon exiting through port L given a particular history H

$$I_{L,H} = \int dx\, \alpha_{L,H}(x) . \qquad (14)$$

Obviously $I_{L,H} + I_{R,H} = 1$, and for single-photon at-a-time scenarios I equals the photon intensity $I = \langle n \rangle$ of Eq. (9).

The effective spatial wavelength Λ for imprint and interrogation can be determined from eq. (10) and is

$$\Lambda = \frac{\lambda}{4 \cdot f \cdot N}\bigg|_{f_{Gauss}\approx 2} \approx \frac{\lambda}{8 \cdot N} , \qquad (15)$$

where the form factor $f = 1$ for a top-hat and roughly two for a Gaussian wave packet [9]. This shrinkage of the effective *imprint* and *interrogation wavelength* Λ is noteworthy, compare plots in Fig. 2 and Fig. 3.

The above kick-factors are special cases of the general back-action a photon imparts onto its scatterer. Typically its back-action destroys coherence [15], but here the interferometer geometrically restricts the photons to two
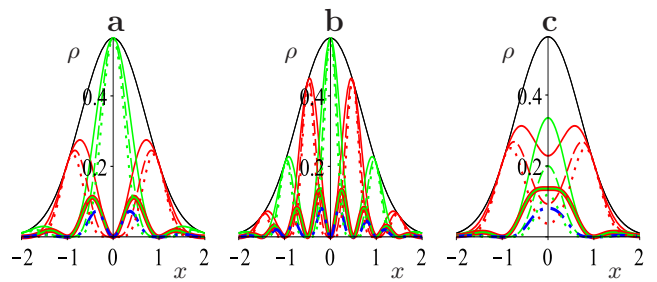
(incoming and two reflected) modes only. We therefore end up with the desirable kick-factors $\mathcal{K}$ that represent controlled, quantum-superposed momentum kicks. This allows us to create Schrödinger cat states from initially stationary quantum mirror states and allows for their detection and reinforcement through quantum entrainment.

For a sufficiently wide coherent quantum mirror wavefunction we end up with sine- or cosine-shaped imprint patterns for $\mathcal{K}_L$ or $\mathcal{K}_R$ respectively. Hence, ρ_L and ρ_R become approximately orthogonal wavefunctions, a second photon γ_s picks up this trace and tends to follow the first photon. This happens with roughly a $75\% : 25\%$ bias, see Fig. 2, the system has thus become quantum entrained. The second photon's detection moreover imprints the same kick-factor onto the quantum mirror's center-of-mass wavefunction thus reinforcing this trend. The third and fourth photons follow their predecessors with an increasing bias of roughly 83% and 87% respectively [9], see Fig. 2 c. Each time, the mirror gets kicked in an identical fashion this procedure reinforces the interference fringes without harm.

All features discussed above prevail for imperfect quantum mirrors even when their reflectivity drops to 60% or less, see Figs. 2 c and 3 c. The rapidity of this method allows us to circumvent the pernicious influences of decoherence and also renders it quite insensitive to the effects of non-zero temperatures of the quantum mirror and non-zero average center-of-mass velocities [9]. The mirror initially has only to provide a sufficiently large coherence length to carry the back-action imprints. Since entrainment happens in the absence of interference patterns the reported effects are also quite insensitive to displacements Δx of the average center-of-mass position of the quantum mirror, as long as $\Delta x \ll c \cdot \delta t$.

An interrogation-photon's arrival time can be delayed in order to allow for investigation of the quantum mirror's time evolution and its decoherence.

An analysis of free photons interacting with a quantum-delocalized mirror inside an interferometer shows that their recoil can create and investigate massive Schrödinger cat states non-destructively, within a picosecond. The analysis shows a new aspect of quantum mechanics – the entrainment of following photons by their predecessors. Quantum entrainment may well turn out to be a useful new response mode of quantum systems in various settings.

[1] W. Heisenberg, Zeitschrift für Physik **43**, 172 (1927).

[2] G. Björk, J. Söderholm, A. Trifonov, T. Tsegaye, and A. Karlsson, Phys. Rev. A **60**, 1874 (1999), arXiv:quant-ph/9904069.

[3] T. J. Kippenberg and K. J. Vahala, Science **321**, 1172 (2008).

[4] V. B. Braginsky and F. Y. Khalili, *Quantum measurement* (Cambridge Univ. Press, Cambridge, 1992).

[5] W. H. Zurek, Rev. Mod. Phys. **75**, 715 (2003).

[6] F. Marquardt and S. M. Girvin, Physics **2**, 40 (2009).

[7] M. Aspelmeyer and K. Schwab, New J. Phys. **10**, 095001 (2008).

[8] T. Corbitt, Y. Chen, E. Innerhofer, H. Müller-Ebhardt, D. Ottaway, H. Rehbein, D. Sigg, S. Whitcomb, C. Wipf, and N. Mavalvala, Phys. Rev. Lett. **98**, 150802 (2007).

[9] O. Steuernagel, *in preparation*.

[10] C. K. Hong, Z. Y. Ou, and L. Mandel, Phys. Rev. Lett. **59**, 2044 (1987).

[11] W. Marshall, C. Simon, R. Penrose, and D. Bouwmeester, Phys. Rev. Lett. **91**, 130401 (2003).

[12] D. Vitali, S. Gigan, A. Ferreira, H. R. Böhm, P. Tombesi, A. Guerreiro, V. Vedral, A. Zeilinger, and M. Aspelmeyer, Phys. Rev. Lett. **98**, 030405 (2007).

[13] S. Huang and G. S. Agarwal, Phys. Rev. A **79**, 013821 (2009), 0810.2589.

[14] K. Jähne, C. Genes, K. Hammerer, M. Wallquist, E. S. Polzik, and P. Zoller, Phys. Rev. A **79**, 063819 (2009), 0904.1306.

[15] O. Steuernagel and H. Paul, Phys. Rev. A **52**, R905 (1995).